

Orbital mixing in CO chemisorption on transition metal surfaces

P. Hu ^{a,1}, D.A. King ^a, M.-H. Lee ^b, M.C. Payne ^b

^a *Department of Chemistry, University of Cambridge, Lensfield Road, Cambridge CB2 1EW, UK*

^b *Cavendish Laboratory, University of Cambridge, Cambridge CB3 0HE, UK*

Received 28 June 1995; in final form 15 September 1995

Abstract

The chemisorption of CO on metal surfaces is widely accepted as a model for understanding chemical bonding between molecules and solid surfaces, but is nevertheless still a controversial subject. Ab initio total energy calculations using density functional theory with gradient corrections for CO chemisorption on an extended Pd(110) slab yield good agreement with experimental adsorption energies. Examination of the spatial distribution of individual Bloch states demonstrates that the conventional model for CO chemisorption involving charge donation from CO 5σ states to metal states and back-donation from metal states into CO 2π states is too simplistic, but the computational results provide direct insight into the chemical bonding within the framework of orbital mixing (or hybridisation). The results provide a sound basis for understanding the bonding between molecules and metal surfaces.

How a molecule bonds to an extended metal surface is a fundamental issue. Chemical bonding in individual molecules and in extended systems such as metals are well understood and documented. However, many aspects of bonding between a molecule and an extended metal surface remain unclear. The chemisorption of CO has been extensively used, both experimentally and theoretically, as a prototype for such studies (see, for example, Ref. [1]). CO is itself, of course, an important molecule in many catalytic reactions on metal surfaces. Despite this, it is still a subject of controversy [2–16]. Using the Hückel molecular orbital approach, Blyholder [2] proposed that a σ -bond is formed between the CO carbon atom and a metal atom, and that further

bonding is provided by the partial filling of the CO π -molecular orbital. This model has become widely accepted, in the form of a synergism between 5σ donation and 2π backdonation. Hoffmann and co-workers [13–15] carried out extended Hückel calculations on CO chemisorption on several metal surfaces and concluded [15] that the Blyholder model is followed in general; but that its major deficiency is the neglect of the 4σ orbital. We note that the authors themselves emphasized the severe limitations of these calculations, and the Blyholder model has been questioned by others [5–8,16].

In order to further understand CO chemisorption, we chose CO chemisorption on Pd(110) and performed ab initio total energy calculations on the system using density functional theory with gradient corrections. A type of Car–Parrinello [17] approach, the conjugate gradients minimisation scheme [18], was used to directly locate electron ground states

¹ Present address: School of Chemistry, Queen's University of Belfast, Belfast BT9 5AG, UK.

[19]. The basis set is composed of plane waves. CO on Pd{110} was modelled using a supercell with three Pd layers and CO molecules placed on one of the two surfaces, at monolayer coverage. We calculated CO on all high symmetry sites of Pd{110} and C–O and C–Pd bond distances were optimised according to forces calculated by the Hellmann–Feynman theorem and total energies. As a sensitive test of the accuracy of this calculation, we reported [20] that the adsorption heat obtained was within 0.15 eV of experiment [21,22]. Details of the calculations are published elsewhere [20,23]. Here we deal specifically with the electronic structure relevant to chemical bond formation at the surface. The geometry of CO chemisorbed on Pd{110} is schematically shown in Fig. 1.

It is well known that eigenstates characterise the main feature of a quantum system. In a molecule, the molecular orbitals are the eigenstates of the system and this is the reason that molecular orbitals, such as the 3σ , 4σ , 1π , 5σ and 2π of CO, are essential to describe the bonding and chemistry of the molecule. In our CO/Pd{110} calculations, total charge densities are obtained as

$$\begin{aligned} \rho_{\text{total}}(\mathbf{r}) &= \sum_{i_{\text{band}}} \sum_{k_j} \rho_{i_{\text{band}}, k_j}(\mathbf{r}) \\ &= \sum_{i_{\text{band}}} \sum_{k_j} |\Psi_{i_{\text{band}}, k_j}(\mathbf{r})|^2, \end{aligned} \quad (1)$$

where i_{band} is a band number; k_j is a k -point; the first and second summations run over all occupied bands and sampled k -points, respectively; and $\Psi_{i_{\text{band}}, k_j}(\mathbf{r})$ is a well-defined Bloch state which is an eigenstate of the extended periodic system. By analogy with the procedure of using molecular orbital

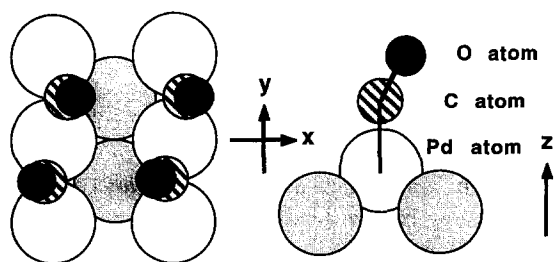


Fig. 1. Schematic illustration of geometry of CO chemisorption on short bridge sites of Pd{110}.

charge density contour plots to understand chemical bonding in molecules, we examined the charge densities of all sampled Bloch states, $\rho_{i_{\text{band}}, k_j}$, for CO/Pd{110}, but only show the charge densities of some Bloch states at the Γ point for CO chemisorption on the symmetric short bridge site. Following this procedure, we find that the valence band structure of CO/Pd{110} can be divided into three sections².

(i) The first section is from the first band (the lowest energy level) to the tenth band; these are CO molecular-orbital-derived levels. The 3σ -derived levels from CO/Pd{110} are very similar to 3σ -derived levels calculated for a CO monolayer raft without a metal substrate, shown in Fig. 2. On the other hand, the 4σ -, 1π - and 5σ -derived levels from CO/Pd{110} also displayed in Fig. 2 very clearly contain the character of specific metal orbitals. The signature of these metal states lies in the shapes of the electron density contour lines. The comparison with the CO raft charge densities provides a clear picture of the influence of metal orbital mixing. We assign the states shown in Figs. 2c, 2e and 2g to bonding states between molecule and surface since there is obviously a charge accumulation between the C end of CO and Pd atoms in the top layer in each state.

(ii) The second valence band section lies between the eleventh band and E_F ; these are metal-derived bands. Interestingly, 4σ , 1π and 5σ character can clearly be observed in this section as well, as shown in Figs. 3a, 3b and 3c, respectively. Crucially, these imply a mixing of 4σ , 1π , and 5σ molecular orbitals of CO with metal bands. Strong 2π character can also be seen, displayed in Fig. 3d, which is assigned to a metal- 2π bonding state between molecule and surface for the same reason stated in the last paragraph.

(iii) The last valence band section lies above E_F . There is strong 5σ and 2π character in this section, as shown in Figs. 3e and 3f, respectively. We assign these two states to metal- 5σ and metal- 2π antibond-

² In our calculations there are two molecules in a unit cell. Thus, ten molecule-derived levels are expected to be seen in the valence band structure. The fortieth band is the highest occupied band at zero temperature.

ing states, respectively, due to nodal planes between molecule and surface.

The above results clearly demonstrate that the notion of charge donation from CO 5σ states to metal states and backdonation from metal states into CO 2π states is oversimplistic. Moreover, the above results broadly provide concrete support for the Hoffmann model, but they do not all sit comfortably with it. The influence of mixing with metal d states on the CO 5π and 2π orbitals is clearly demonstrated in Fig. 2g and Fig. 3d. However, the 1π -derived CO/Pd orbital contains metal character; and

the metal-derived bands contain strong 5σ and some 4σ and 1π character. These findings can, nevertheless, be rationalised within the orbital mixing model schematically shown in the form of a correlation diagram in Fig. 4. Valence bands of a clean metal surface are represented on the left hand side; discrete levels for gaseous CO are shown on the right hand side; and CO chemisorption on the metal surface is displayed in the centre. We divide the molecular orbitals of CO into three groups. The first group, containing only the 3σ orbital, hardly interacts with the metal bands due to low lying energy level, and is

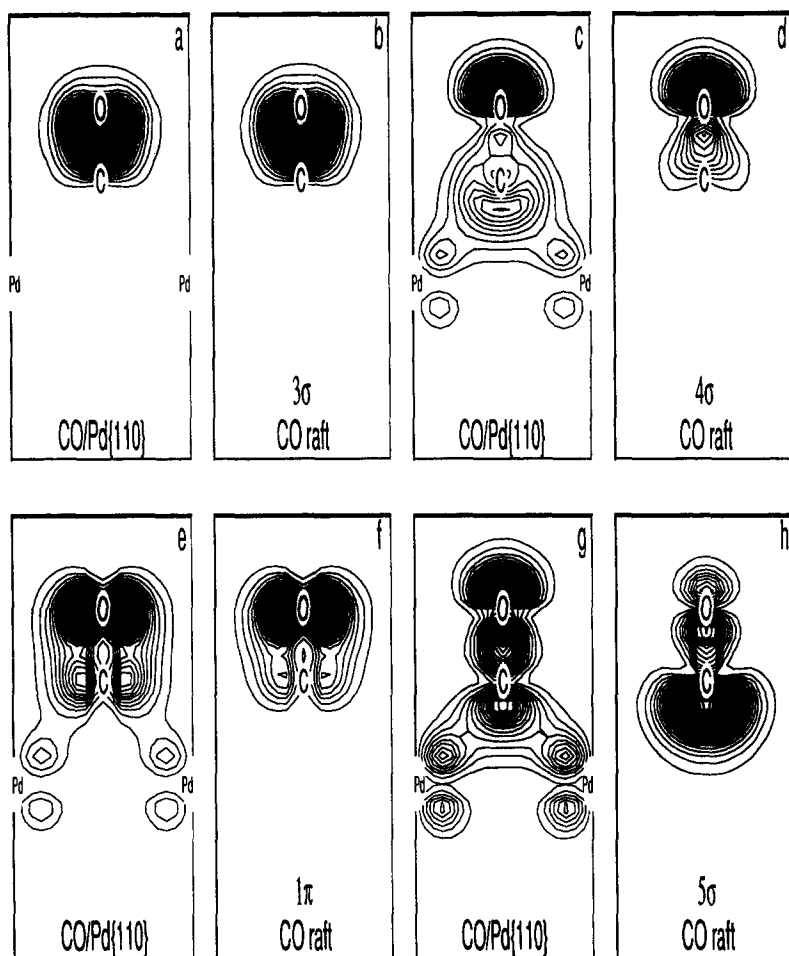


Fig. 2. A charge density comparison of 3σ -, 4σ -, 1π - and 5σ -derived orbitals between CO/Pd(110) and CO monolayer without metal. (a), (c), (e) and (g) are 2D contours of charge densities of 3σ -, 4σ -, 1π - and 5σ -derived orbitals respectively, cut through the C–O and C–Pd bond axes, which correspond to $\rho_{i_{\text{band}}, k_j}$ from CO/Pd(110) at $k_j = \Gamma$, $i_{\text{band}} = 2$ (-23.86 eV), 4 (-9.23 eV), 10 (-5.41 eV) and 7 (-6.99 eV), respectively, where E_F is defined as zero. O, C and top layer Pd atom positions are labelled. (b), (d), (f) and (h) are the same but from CO monolayer without metal, which correspond to $\rho_{i_{\text{band}}, k_j}$ at $k_j = \Gamma$, $i_{\text{band}} = 2, 4, 8$ and 10 , respectively.

essentially not involved in chemisorption. The second group containing the 4σ and 1π orbitals is mixed with the metal bands, particularly the d bands, but all the levels so formed lie below E_F and the net contribution to the chemisorption energy is very small. The third group containing the 5σ and 2π orbitals is, however, sufficiently strongly mixed to produce unfilled antibonding states above E_F which therefore provide significant net bonding to the sur-

face. Consequently, 4σ -, 1π - and 5σ -derived levels contain metal orbital character; and metal-derived levels themselves contain strong 5σ , 2π and some 4σ , 1π character. The main metal- 5σ and metal- 2π antibonding states are located above E_F .

The model specifically includes the band structure of the metal surface. We do not specifically distinguish between the interaction of the CO 5σ orbital with metal d orbitals and CO 5σ with metal s or p

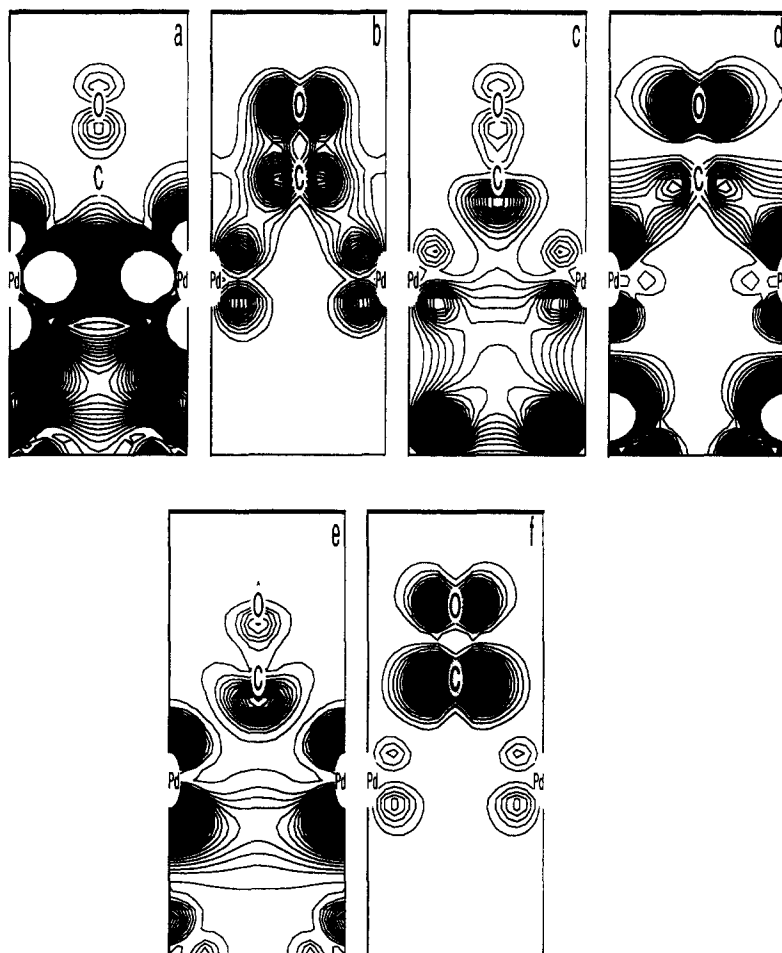


Fig. 3. Illustration of 4σ , 1π , 5σ and 2π character in metal-derived bands and metal- 5σ and metal- 2π antibonding states. (a), (b), (c) and (d) are the same cuts as Fig. 2a but from $\rho_{i_{\text{band}}, k_j}$ at $k_j = \Gamma$, $i_{\text{band}} = 11$ (-4.72 eV), 12 (-4.30 eV), 16 (-3.97 eV) and 34 (-0.85 eV) respectively, showing 4σ , 1π , 5σ and 2π character in the metal-derived bands, respectively. The absolute intensities in (b) are similar to the absolute intensities near C and O atom positions in (a), but the absolute intensities in other regions such as the second layer of Pd are much higher. Similar features in (c) and (d) can be found at $i_{\text{band}} = 13$ (-4.19 eV), 18 (-3.30 eV), 29 (-1.56 eV), 30 (-1.21 eV) and 17 (-3.86 eV), 20 (-3.11 eV), 24 (-2.47 eV), 32 (-1.17 eV), 36 (-0.52 eV), respectively. (e) and (f) are the same cuts but from $\rho_{i_{\text{band}}, k_j}$ at $k_j = \Gamma$, $i_{\text{band}} = 42$ (1.29 eV) and 50 (3.71 eV), respectively, which are above the Fermi level, showing metal- 5σ and metal- 2π antibonding states, respectively.

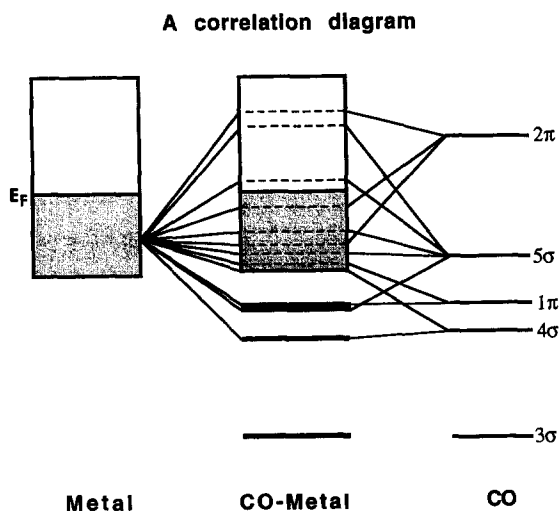


Fig. 4. Schematic illustration of the orbital mixing model.

orbitals, although we expect the latter to make a relatively small bonding contribution. Obviously, the metal energy levels, shown in Fig. 4, play a decisive role in CO chemisorption. One of the reasons for weak CO chemisorption on Cu surfaces may be that all d bands are below E_F (the highest d band is about 1.5 eV below E_F). Consequently, on Cu all metal d–5 σ antibonding states will be below E_F , reducing the net contribution from 5 σ to metal–CO bonding. Furthermore, the reduction of the interaction between metal valence bands and the CO 2 π orbitals is partially due to the shift of CO to the atop position of Cu, where it minimises the repulsive interaction between the 5 σ and Cu 3d orbitals. From experiments it is well known that CO adsorption tends to be dissociative on the left hand side of the first-row transition metals; but non-dissociative on the right hand side [13,24]. As the transition metal substrate is switched from Cu at the right to, say, Fe towards the left hand side of the periodic table, the d band energy levels shift upwards. This results in an increased overlap of metal d states with the CO 2 π orbital, leading, in particular, to an increase in population of Bloch states containing the CO 2 π feature, such as that shown in Fig. 3d, which have C–O antibonding character. This leads to a weakening of the CO bond, and weakening of this bond can lead to CO dissociation. Similar arguments have been used by Hoffmann and co-workers [13].

In summary, we have displayed individual Bloch states for CO chemisorption on an extended metal surface in real space. Examination of the spatial symmetry characteristics of the charge distribution in these states provides a ready means of identification and assignment of bonding and antibonding character, which demonstrates that the Blyholder model is oversimplistic. We have divided the band structure of CO/Pd{110} into three sections and CO molecular orbitals into three groups. Their individual roles in CO chemisorption are explicitly discussed. The description of CO chemisorption which emerges provides a sound basis for fully characterising bonding between molecules and metal surfaces.

Acknowledgement

Parts of these calculations were performed at the parallel processor machine at Daresbury, UK. We acknowledge EPSRC for an equipment grant and a Postdoctoral Research Fellowship to PH and for supporting the work of M-HL and MCP.

References

- [1] J.C. Campuzano, in: *The chemical physics of solid surfaces and heterogeneous catalysis*, Vol. 3A, eds. D.A. King and D.P. Woodruff (Elsevier, Amsterdam, 1990) p. 389.
- [2] G. Blyholder, *J. Phys. Chem.* 68 (1964) 2772.
- [3] G. Blyholder and M.C. Allen, *J. Am. Chem. Soc.* 91, (1969) 3158.
- [4] E. Wimmer, C.L. Fu and A.J. Freeman, *Phys. Rev. Letters* 55 (1985) 2618.
- [5] S. Ishi, Y. Ohno and B. Viswanathan, *Surface Sci.* 161 (1985) 349.
- [6] Ph. Avouris, *Phys. Scripta* 35 (1987) 47.
- [7] B. Gumhalter, K. Wandelt and Ph. Avouris, *Phys. Rev. B* 37 (1988) 8048.
- [8] P.S. Bagus, C.J. Nelin and C.W. Bauschlicher Jr., *Phys. Rev. B* 28 (1983) 5423.
- [9] G. Pacchioni and J. Koutecky, *J. Phys. Chem.* 91 (1987) 2658.
- [10] M.E. Grillo, G.K. Castro and G. Doyen, *J. Chem. Phys.* 97 (1992) 7786.
- [11] R.J. Smith, J. Anderson and G.J. Lapeyre, *Phys. Rev. B* 22 (1980) 632.
- [12] R. Miranda, K. Wandelt, D. Rieger and R.D. Schnell, *Surface Sci.* 139 (1984) 430.
- [13] S.-S. Sung and R. Hoffmann, *J. Am. Chem. Soc.* 107 (1985) 578.

- [14] J. Li, B. Schiott, R. Hoffmann and D.M. Proserpio, *J. Phys. Chem.* **94** (1990) 1554.
- [15] Y.-T. Wong and R. Hoffmann, *J. Phys. Chem.* **95** (1991) 859.
- [16] M.C. Zonnevylle, J.J.C. Geerlings and R.A. van Santen, *J. Catal.* **148** (1994) 417.
- [17] R. Car and M. Parrinello, *Phys. Rev. Letters* **55** (1985) 2471.
- [18] M.P. Teter, M.C. Payne and D.C. Allen, *Phys. Rev. B* **40** (1989) 12255.
- [19] M.C. Payne, M.P. Teter, D.C. Allen, D.C. Arias and J.D. Joannopoulos, *Rev. Mod. Phys.* **64** (1992) 1045.
- [20] P. Hu, D.A. King, S. Crampin, M.-H. Lee and M.C. Payne, *Chem. Phys. Letters* **230** (1994) 501.
- [21] R. Raval, S. Haq, M.A. Harrison, G. Blyholder and D.A. King, *Chem. Phys. Letters* **167** (1990) 391.
- [22] P. Hu, L.M. de la Garza, R. Raval and D.A. King, *Surface Sci.* **249** (1991) 1.
- [23] P. Hu, D.A. King, M.-H. Lee, S. Crampin and M.C. Payne, *Phys. Rev. B*, submitted for publication.
- [24] G. Broden, T.N. Rhodin, C. Brucker, R. Benbow and Z. Hurych, *Surface Sci.* **59** (1976) 593.